© 2016. Published by The Company of Biologists Ltd | Development (2016) 143, 4701-4712 doi:10.1242/dev.138719

RESEARCH ARTICLE

Delayed neurogenesis with respect to eye growth shapes the pigeon retina for high visual acuity

Tania Rodrigues[1], Michal Krawczyk[2], Dorota Skowronska-Krawczyk[1,*], Lidia Matter-Sadzinski[1] and Jean-Marc Matter[1,‡]

ABSTRACT

The macula and fovea located at the optical centre of the retina make primate visual perception unique among mammals. Our current understanding of retina ontogenesis is primarily based on animal models having no macula and no fovea. However, the pigeon retina and the human macula share a number of structural and functional properties that justify introducing the former as a new model system for retina development. Comparative transcriptome analysis of pigeon and chicken retinas at different embryonic stages reveals that the genetic programmes underlying cell differentiation are postponed in the pigeon until the end of the period of cell proliferation. We show that the late onset of neurogenesis has a profound effect on the developmental patterning of the pigeon retina, which is at odds with the current models of retina development. The uncoupling of tissue growth and neurogenesis is shown to result from the fact that the pigeon retinal epithelium is inhibitory to cell differentiation. The sum of these developmental features allows the pigeon to build a retina that displays the structural and functional traits typical of primate macula and fovea.

KEY WORDS: Avian transcriptome, Retinal ganglion cell, Photoreceptor, Notch signalling, Atonal homolog 7, Fibroblast growth factor 3, Neurogenin 2

INTRODUCTION

Primate retinas are characterised by a specialised central region, the macula, while their periphery resembles that of other mammals. The macula is subdivided into different areas, including the fovea and the foveola. The latter is located in the centre of the fovea, is devoid of rods and contains only cones. The neuronal composition of the fovea favours neurons of the midget pathway, a circuit essential for high visual acuity and colour vision, consisting of one cone that forms synapses with two bipolar cells, which in turn make connections with two retinal ganglion cells (RGCs). About half of the 1.2×10^6 RGCs in the human retina are located in the fovea, which represents less than 1% of the total retinal surface (Kolb, 1995). The macula and fovea make primate visual perception unique among mammals. An understanding of the genetic network underlying the development and maintenance of this highly specialised region is instrumental to addressing issues about human macula-related retinopathies, yet our current knowledge of retina ontogenesis is primarily based on animal models that have no macula and no fovea. With a RGC:rod ratio of ∼1:100, the mouse retina resembles the peripheral retina of primates. The ratio of RGCs to photoreceptors is higher in the chicken retina but the density of RGCs in the area centralis is still much lower than at the foveal rim in the human macula (∼14×10^3 versus ∼60×10^3 RGCs/mm^2 in chicken versus human).

The transcription factor (TF) atonal homolog 7 (ATOH7; also known as ATH5) is required for the production of RGCs in vertebrates (Brown et al., 2001; Del Bene et al., 2007; Kanekar et al., 1997; Kay et al., 2001; Liu et al., 2001; Matter-Sadzinski et al., 2001; Wang et al., 2001) and the transcriptional network underlying the production of RGCs is well conserved between mouse, chicken and fish (Brown et al., 1998, 2001; Hufnagel et al., 2010; Kay et al., 2001; Matter-Sadzinski et al., 2001, 2005; Sinn et al., 2014; Skowronska-Krawczyk et al., 2004, 2009). However, whereas the majority of the ATOH7-expressing cells enter the RGC lineage in the chick, only a few percent produce RGCs in the mouse (Prasov and Glaser, 2012; Skowronska-Krawczyk et al., 2009; Yang et al., 2003). Sustained expression of ATOH7 is required during the last cell cycle for cells to enter the RGC lineage. In chick, efficient NGN2-mediated activation of *Atoh7* transcription, *Atoh7* autostimulation and HES5.3-mediated lengthening of the cell cycle increase the proportion of cells that enter this lineage (Chiodini et al., 2013; Skowronska-Krawczyk et al., 2009). However, this still does not result in numbers of RGCs as high as in the macula and fovea (Fig. 1).

The retinas of flying birds have high acuity regions, with one and sometimes two foveae. The pigeon has two regions of high RGC density and one fovea (Fig. 1) (Galifret, 1968; Querubin et al., 2009) and the visual acuity of the pigeon and human eyes are comparable (Hodos and Leibowitz, 1977; Williams, 1985). This prompted us to introduce the pigeon as a new model system for analysing retina development. Our study uncovers that by deferring neurogenesis to the end of the period of cell proliferation, the pigeon has developed an effective way to expand the pool of progenitor cells that enter the RGC lineage, thereby increasing the density of RGCs and the number of optic nerve axons in the adult eye. We further show that, although neurogenesis proceeds according to different schedules in pigeon and chick, retinas grow at a similar pace in both species. Moreover, the developmental patterning of the pigeon retina differs from the current models of retina development, which are largely based on studies performed with chick, mouse and fish embryos. Our study reveals that mechanisms exist for the eye of vertebrates to disconnect tissue growth and cell differentiation, allowing the pigeon to develop a retina that displays structural and functional features of macula and fovea.

[1]Department of Molecular Biology and Department of Biochemistry, Sciences III, University of Geneva, 30 quai Ernest-Ansermet, 1211 Geneva 4, Switzerland. [2]Shiley Eye Institute, Department of Ophthalmology, University of California, San Diego, La Jolla, CA 92093, USA.
*Present address: Shiley Eye Institute, Department of Ophthalmology, University of California, San Diego, La Jolla, CA 92093, USA.

‡Author for correspondence (jean-marc.matter@unige.ch)

J.-M.M., 0000-0002-2906-2462

Received 18 April 2016; Accepted 1 November 2016

Development (2016) 143, 4701-4712 doi:10.1242/dev.138719

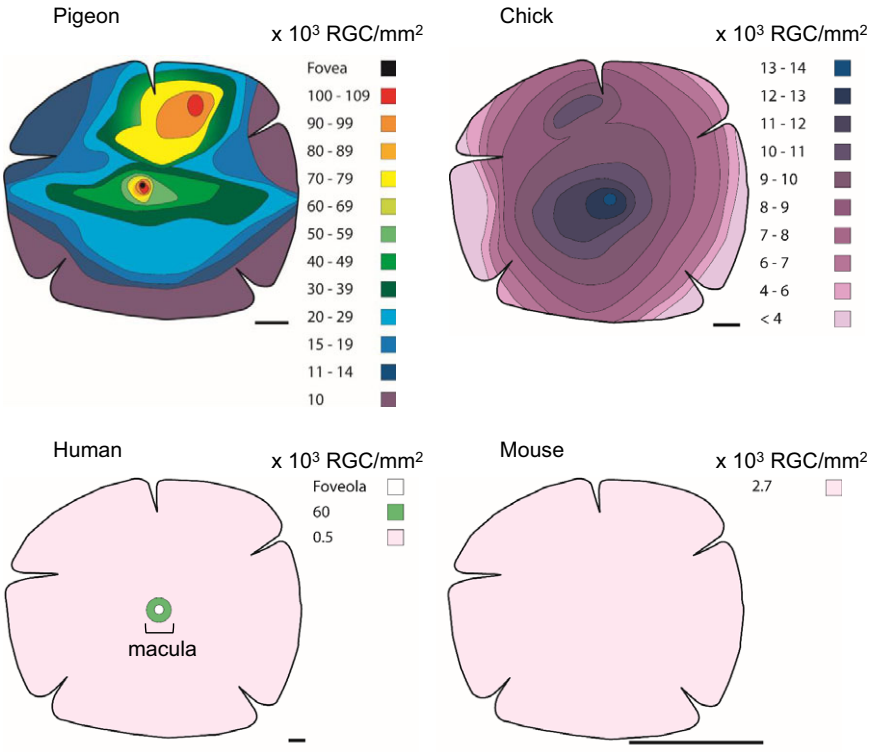

Fig. 1. Topographic maps showing RGC densities in flat-mount retinas. The variations in RGC densities throughout the central and peripheral areas of adult pigeon, chicken, mouse and human retinas are colour coded. In pigeon, the central perifoveal area and the dorso-peripheral area (red field) are two regions of high RGC density. In chicken, there is an area centralis (Bruhn and Cepko, 1996). The RGC density is ~8-fold higher in the pigeon fovea than in the chicken area centralis (Chen and Naito, 1999; Querubin et al., 2009). In human, the RGC density in the tiny perifoveal region is comparable to that of the pigeon, whereas the very low RGC density outside this region is in a range comparable to that of mouse. The pigeon and chick data were redrawn from Querubin et al. (2009) and Chen and Naito (1999), respectively. Human and mouse data are from Conradi and Sjöstrand (1993) and Jeon et al. (1998), respectively. Scale bars: 2 mm.

RESULTS

Eye growth and retina development in pigeon and chick

Analysis of pigeon (*Columba livia*) and chick (*Gallus gallus*) at equivalent embryonic developmental stages (Fig. S1A) revealed no striking difference in eye development. Measuring the surface of the retina (Fig. 2A), the number of retinal cells (Fig. 2B) and the number of cell divisions per day (Fig. 2C) indicated that pigeon and chick retinas grow and expanded at a similar pace. The cell division rates were remarkably close in both species from embryonic day (E) 4 to 8. The average rate of cell division during this period (Fig. 2C) is consistent with cell cycles that last 11-15 h (Chiodini et al., 2013). By E8, the majority of cells had been produced in pigeon and chick, and the number of cells increased modestly in both species between E8 and E10 (Fig. 2B).

Despite the fact that the retinas grew at a similar pace in the two species, we noted significant differences in the histology of the retinas at equivalent embryonic ages (Fig. 2D). Whereas at E9 the outer nuclear layer (ONL) bearing the cone and rod photoreceptors, the inner nuclear layer (INL) bearing the bipolar, amacrine and horizontal cells, and the ganglion cell layer (GCL) bearing RGCs and displaced amacrine cells, were already well developed in the central and peripheral chick retina, these layers were indiscernible in the E9 pigeon retina (Fig. 2D). Retinal lamination became visible in the pigeon central retina at ~E10 and the retinas of both species looked similar at ~E12, with some notable differences. In pigeon, the nerve fibre layer (NFL) that contains RGC axons is much thicker and the ratio of GCL cells to ONL cells is ~4-fold higher than in chick (Fig. S1B, Fig. S2).

Comparative transcriptome analysis reveals delayed cell differentiation in the pigeon retina

Intrigued by the 3-day delay in the development of the retinal layers in pigeon, we wondered whether it reflected a delay in neurogenesis. In the current animal models, RGCs are the first neurons to be born and they appear shortly after the formation of the optic cup. In chick, the first *Atoh7*-expressing cells and the first RGCs with growing axons are detected at E2 and E2.5, respectively (Goldberg and Coulombre, 1972; Matter-Sadzinski et al., 2005; McCabe et al., 1999; Prada et al., 1991), whereas in pigeon they were detected at E5 and E5.5, respectively (Fig. 3A). Axon counting in the developing optic nerve is a direct and unequivocal method to monitor the dynamics of RGC differentiation. Whereas axon number peaks in chick at E10 (Rager, 1980), only ~20% of the final number of axons were counted at this stage in pigeon (Fig. 3B). The expression profile of *Atoh7* was analysed by northern blot and real-time quantitative PCR (RT-qPCR). In pigeon, *Atoh7* mRNA was first detected at E6 and transcript accumulation peaked between E8 and E10, 3 days later than in the chick (Fig. 3C,D). Consistent with the fact that NGN2 activates transcription of the *Atoh7* gene (Hufnagel et al., 2010; Matter-Sadzinski et al., 2005; Skowronska-Krawczyk et al., 2009), *Ngn2* expression was also delayed in pigeon (Fig. 3E). The observation that *Ngn2* and *Atoh7* expression peaked at the end of the period of cell proliferation in pigeon, whereas it culminated when cells were still rapidly dividing in chick (Fig. 2C), suggests that proneural gene expression is not coordinated with the rate of cell division.

Since the timing of RGC differentiation differs between pigeon and chick, we examined the extent to which the development of the whole retina varies between the two species. We compared the diversity and dynamics of the pigeon and chick RNA-Seq transcriptomes at three critical stages: (1) E3-E3.5 (referred to as E3), encompassing the onset of neuronal differentiation in chick; (2) E5-E5.5 (referred to as E5), encompassing the onset of neuronal differentiation in pigeon and the peak of *Atoh7* expression in chick; (3) and E8-E8.5 (referred to as E8), which encompasses the upregulation of *Atoh7* in pigeon. RNA samples were isolated in triplicate at each stage and the 18 samples were processed for transcriptome analysis by RNA-Seq. In order to organise the large

Development (2016) 143, 4701-4712 doi:10.1242/dev.138719

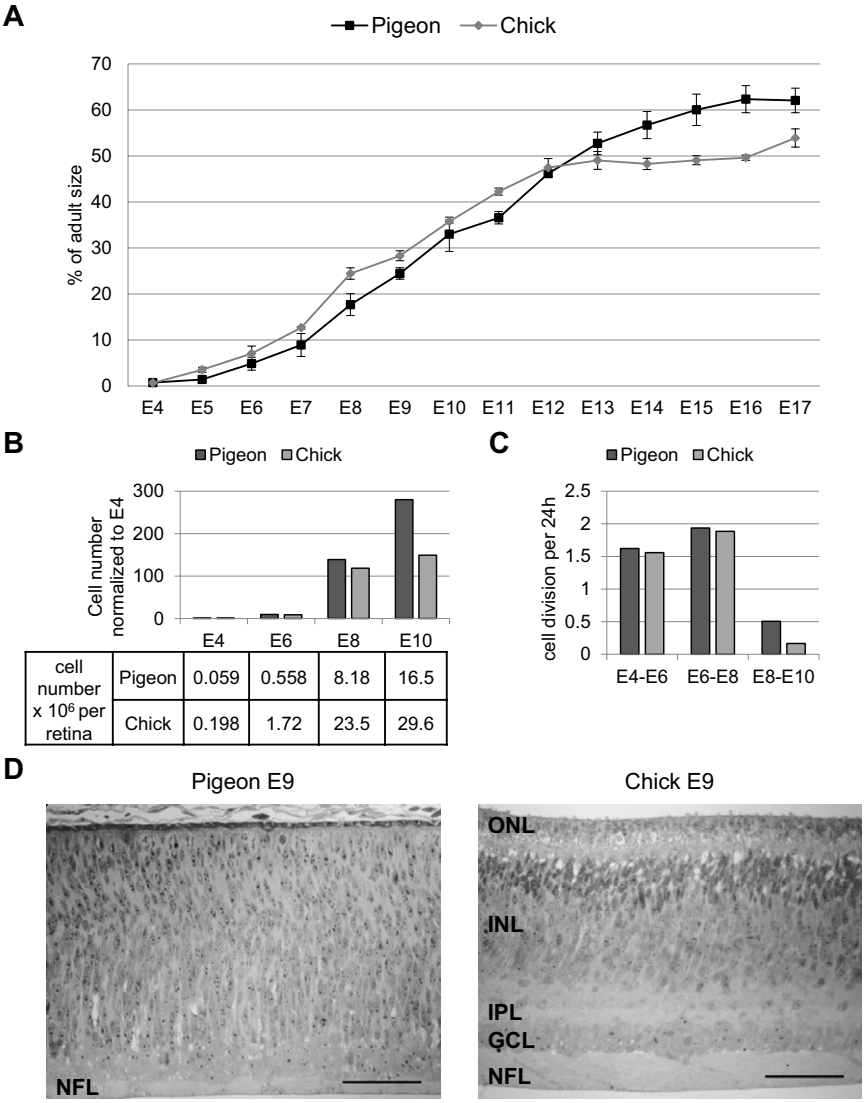

cell number x 10^6 per retina					
	Pigeon	0.059	0.558	8.18	16.5
	Chick	0.198	1.72	23.5	29.6

Fig. 2. Growth rates and development of the pigeon and chick retinas. (A-C) Comparative measurements of retina surface area (A), cell number per retina (B) and number of cell divisions per 24 h (C). In B and C, cell counting is from independent experiments ($n \geq 4$) performed in parallel on the pigeon and chick retinas. At each developmental stage, data are from three biological replicates and presented as mean±s.d. In B, s.d. ≤13%. (D) Semi-thin tissue sections from the central retina. In chick, retinal lamination is already well developed. In pigeon, the nuclear and plexiform layers are not yet visible, except for the NFL. ONL, outer nuclear layer; INL, inner nuclear layer; IPL, inner plexiform layer; GCL, ganglion cell layer; NFL, nerve fibre layer. Scale bars: 50 µm.

amount of data, we ordered genes according to their expression profiles in chick using the three paired embryonic stage comparisons: E3-E5, E5-E8 and E3-E8. Because our aim was to identify genes that participate in early retina development, we selected among the transcripts and the corresponding genes those that displayed significant fold changes (≥1 and ≤−1 in $\log_2$) in chick between E3 and E5. This set represents ∼36% of the compendium of chicken genes that we selected and is referred to as 1/N/N. About 75% of these genes showed different expression profiles in pigeon and chick (Table S1). A heat map generated with clustered genes upregulated or downregulated between E3 and E5 in chick revealed that ∼64% of the corresponding genes in pigeon did not show significant variation in expression during this early period; instead, their expression changed between E5 and E8 (Fig. S3A).

To determine whether this delay reflected the late onset of RGC differentiation in pigeon, we focused our analysis on genes regulated by ATOH7 (Fig. S3B). About 95% of such genes were upregulated between E3 and E5 in chick. By contrast, pigeon orthologues were activated or displayed stronger activation between E5 and E8. The delayed onset of expression of ATOH7-regulated genes in pigeon and, in particular, of the ATOH7 target genes involved in axonal outgrowth and neuronal activity (Fig. S3C; e.g. *Stmn2*, *Chrnb3*, *Ptn*) (Chiodini et al., 2013; Skowronska-Krawczyk et al., 2009), indicates that neuronal differentiation is delayed in pigeon. Deferred expression of TFs that exert control over photoreceptor, amacrine, horizontal and bipolar cell specification (Fig. S3C) is reflected in the delayed development of the ONL and INL (Fig. 2D). Taken together, our data suggest that cell differentiation into most types of retinal neurons is postponed in pigeon.

The genetic programme underlying retina growth unfolds at the same pace in pigeon and chick

About 25% of the selected 1/N/N set of genes displayed the same expression profiles in the three paired embryonic stage comparisons of the two species. These included the core cell cycle regulators cyclin A1 and cyclin D2, the TFs *Sox2*, *Klf5* and *c-Myc* and the tumour suppressor *p63* (*Tp63*) (Fig. 4E, Table S1), providing further evidence that cell cycle progression and the dynamics of progenitor cell expansion proceeded at the same pace in pigeon and chick up to E8. Moreover, 12 genes encoding TFs and transcriptional regulators displayed identical expression profiles in both species, suggesting that they regulate aspects of retina morphogenesis that develop independently of neurogenesis and

Development (2016) 143, 4701-4712 doi:10.1242/dev.138719

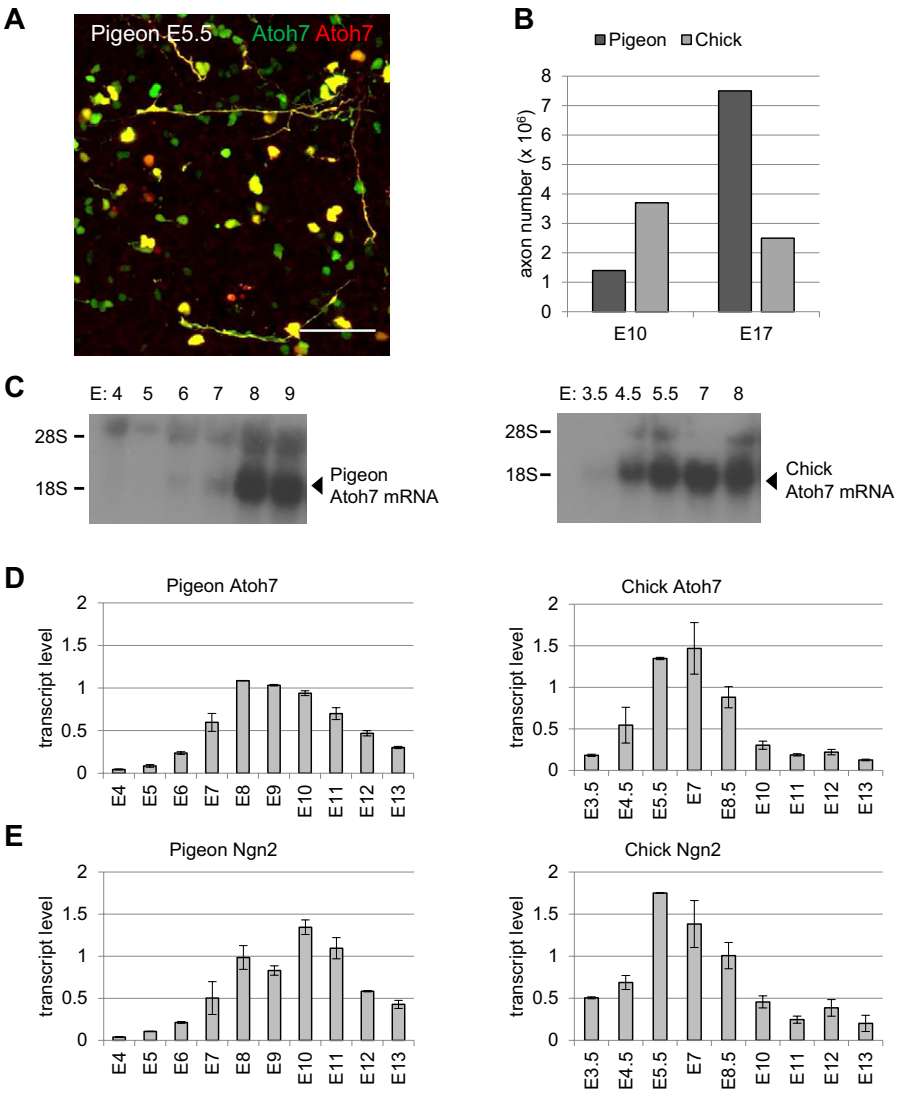

Fig. 3. Delayed onset of RGC differentiation in the pigeon. (A) E5 pigeon retinas co-electroporated with Atoh7-GFP and Atoh7-RFP. Atoh7-RFP specifically identifies newborn RGCs (Chiodini et al., 2013). The first double-labelled RGCs and axons were detected in the central and peripheral retina 12 h after electroporation. (B) Axon numbers in pigeon and chick optic nerves. For pigeon, mean values obtained with two optic nerves at each stage are shown. The chick data are from Rager (1980). (C) Accumulation of *Atoh7* mRNA detected by northern blot. (D,E) Accumulation of *Atoh7* and *Ngn2* transcripts measured by RT-qPCR analysis. At each developmental stage, data are from three biological replicates and presented as mean±s.d.

cell differentiation (Fig. 4E). Comparative morphological analysis (Fig. 4A-D) indicated that the curvature of the retinal epithelium, the closure of the optic fissure and the formation of the optic disc developed at a similar pace in both species.

Cell adhesion, matrix and matrix-associated proteins help establish the static aspects of epithelial architecture and are thought to participate in epithelial cell dynamics, driving the morphogenetic events that shape the retina. Genes encoding cell adhesion and matrix proteins and displaying the same expression profiles in pigeon and chick (Fig. 4F) could be driving those epithelial morphogenesis processes that are independent of cell differentiation. By contrast, other genes encoding matrix or cell adhesion components displayed early variations in expression in chick, but not in pigeon, suggesting that they might play a role in cell differentiation (Fig. 4G). In sum, our transcriptome comparison revealed that parts of the genetic programme underlying retina development progress independently of cell differentiation.

Delaying neuronal differentiation as an adaptation for increasing RGC numbers

We asked whether the delayed neuronal differentiation had an effect on the total number of RGCs produced in pigeon. At the peak of *Atoh7* expression, ~5% and ~50% of the total number of progenitor cells had been generated in chick and pigeon retinas, respectively (Fig. 2B), while the RT-qPCR analysis indicated that the accumulation of *Atoh7* transcripts was similar in both species (Fig. 3D). To improve the accuracy of this estimate, we measured the number of *Atoh7* transcripts per microgram of total RNA using a counter analysis system from NanoString Technologies. The counts of *Atoh7* transcripts were remarkably similar in E5.5 to E6 chick and in E8 to E10 pigeon retinas (Fig. 5A), suggesting that the accumulation of *Atoh7* transcripts depends neither on the number of cell divisions nor on the size of the retina. Taking into account the differences in RNA content at the peak of *Atoh7* expression (Fig. 5C), the number of *Atoh7* transcripts per retina was ~3-fold higher in pigeon (Fig. 5D,E).

To compare the proportions of cells that entered the RGC lineage at the peak of *Atoh7* expression, E6 chick and E9 pigeon retinal cells were transfected with the Atoh7-RFP and CMV-GFP reporters and fluorescent cells were counted 24 h later (Fig. 5B). Atoh7-RFP identifies cells expressing *Atoh7* at high level and that enter the RGC lineage (Chiodini et al., 2013). We calculated the fractions of *Atoh7*-expressing cells, and we estimated that in pigeon three times as many cells entered the RGC lineage during this 24-h period (~1.26×10^6 versus ~0.43×10^6 cells/retina in pigeon versus chick; Fig. 5C,E). This difference matches the 2- to 3-fold higher cell

Development (2016) 143, 4701-4712 doi:10.1242/dev.138719

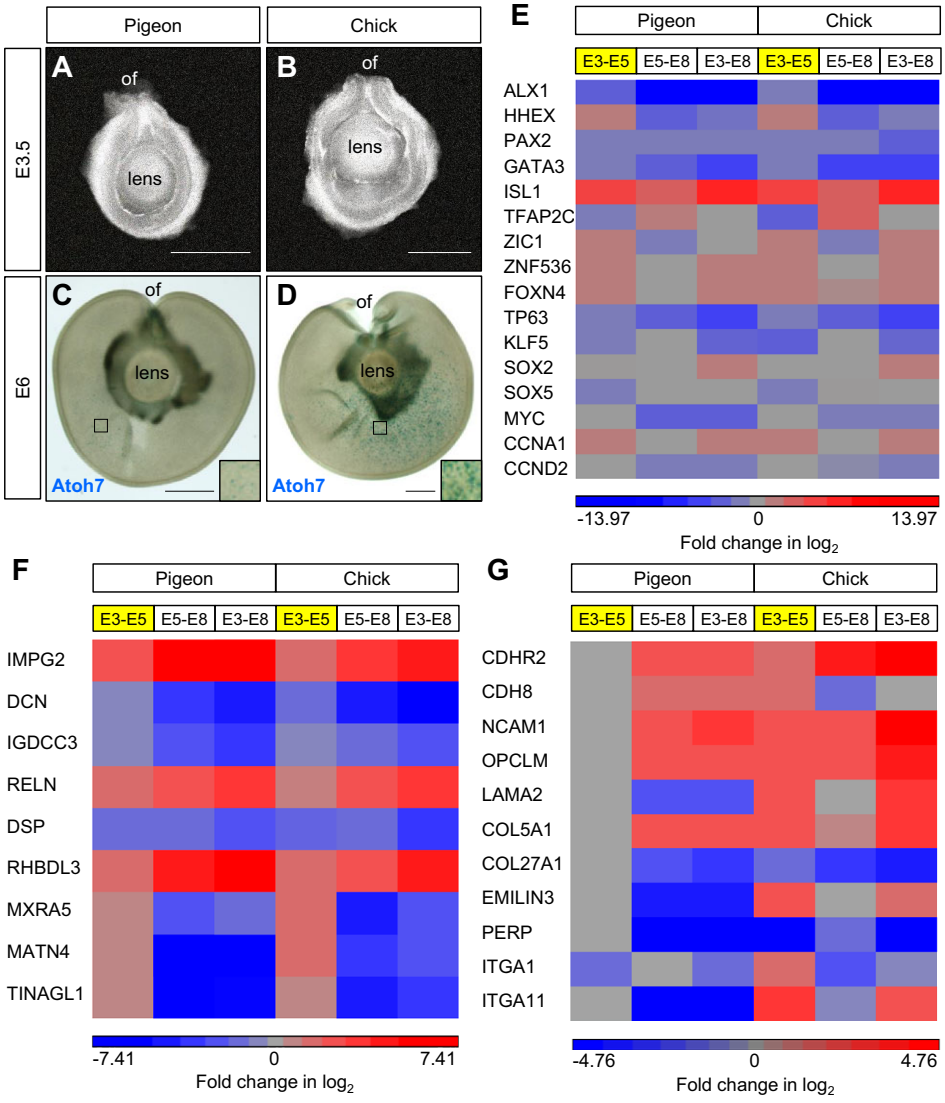

Fig. 4. The genetic programme underlying retina growth progresses independently of cell differentiation. (A-D) Comparison of the shape of the retina and of the closure of the optic fissure (of) at E3.5 (A,B) and E6 (C,D). (C,D) E6 retinas were electroporated with Atoh7-lacZ and stained for β-galactosidase 24 h later. In pigeon, rare blue cells are scattered throughout mid-peripheral areas. Boxed regions are magnified in the insets. The eye lens and retinal pigmented epithelium fragments are apparent by retina transparency. Scale bars: 500 µm. (E-G) Heat maps generated from RNA-Seq data with genes encoding TFs and cell cycle regulators (E), cell adhesion, matrix and matrix-associated proteins (F,G) that display the same (E,F) or different (G) expression profiles in pigeon and chick.

density in the pigeon GCL at E12 (Fig. S2) and the 3-fold difference in the number of optic nerve axons between the two species at E17 (Fig. 3B, Fig. 5E). Likewise, in the days following the peak of *Atoh7* expression, the density of RGCs reached ~70×10^3 cells/mm^2 and these neurons were uniformly distributed throughout the retina, except for modest increases in density in the central area (Fig. S2). After cessation of mitotic activity, the retinal surface area increased by a factor of two (~110 mm^2 at E12 versus ~250 mm^2 1 year post hatching). We suppose that the different RGC densities (7-10×10^4 cells/mm^2 in the perifoveal and red field areas versus 1-3×10^4 cells at the periphery; Fig. 1) are established during this period of expansion.

In pigeon, RGCs and photoreceptors have congruent periods of genesis and there is no central-to-peripheral gradient in their emergence

Both species displayed the same high rate of cell division from E4 to E8, followed by a rapid decrease in cell divisions between E8 and E10 (Fig. 2C). However, analysis of the distribution of cells pulsed with BrdU for 1 h at E9 revealed a remarkable difference in the spatial distribution of dividing cells between the pigeon and chick retinas. According to the classical model, which is mostly based on chicken and mouse studies, the retina develops in a centro-peripheral sequence; that is, cessation of cell division occurs first in the central area and then extends to the periphery (Hufnagel and Brown, 2013; Prada et al., 1991). It appears that this model does not apply to the pigeon retina, where dividing cells are evenly distributed throughout the central and peripheral areas up to E9. The fact that the total number of cells doubled in the pigeon retina between E8 and E10 (~8.2×10^6 at E8 versus ~16.5×10^6 at E10; Fig. 2B) and that 40±5% of cells were in S phase in the central and peripheral retina at E9 (Fig. 6A; data not shown) suggest that the vast majority of cells did progress through cell cycles that lasted more than 24 h at this stage of development. In line with this idea, the majority of BrdU-labelled nuclei displayed sparse fluorescence puncta (Fig. 6A, inset), suggesting that they had a decreased number of replication foci and that cells progressed through a long S phase (Duronio, 2012). At E12, <1% of pigeon cells were in S phase (Fig. 6B) and $35\pm3\times10^6$ cells per retina were counted.

To determine whether the pigeon retina displays a class-specific sequence of birth dates and a central-to-peripheral gradient in genesis, BrdU was injected *in ovo* at E6, E8, E9 or E10 and the retinas were processed for immunohistochemistry analysis at E12. The label was detected in the nuclei of cells that were about to be born at the

Development (2016) 143, 4701-4712 doi:10.1242/dev.138719

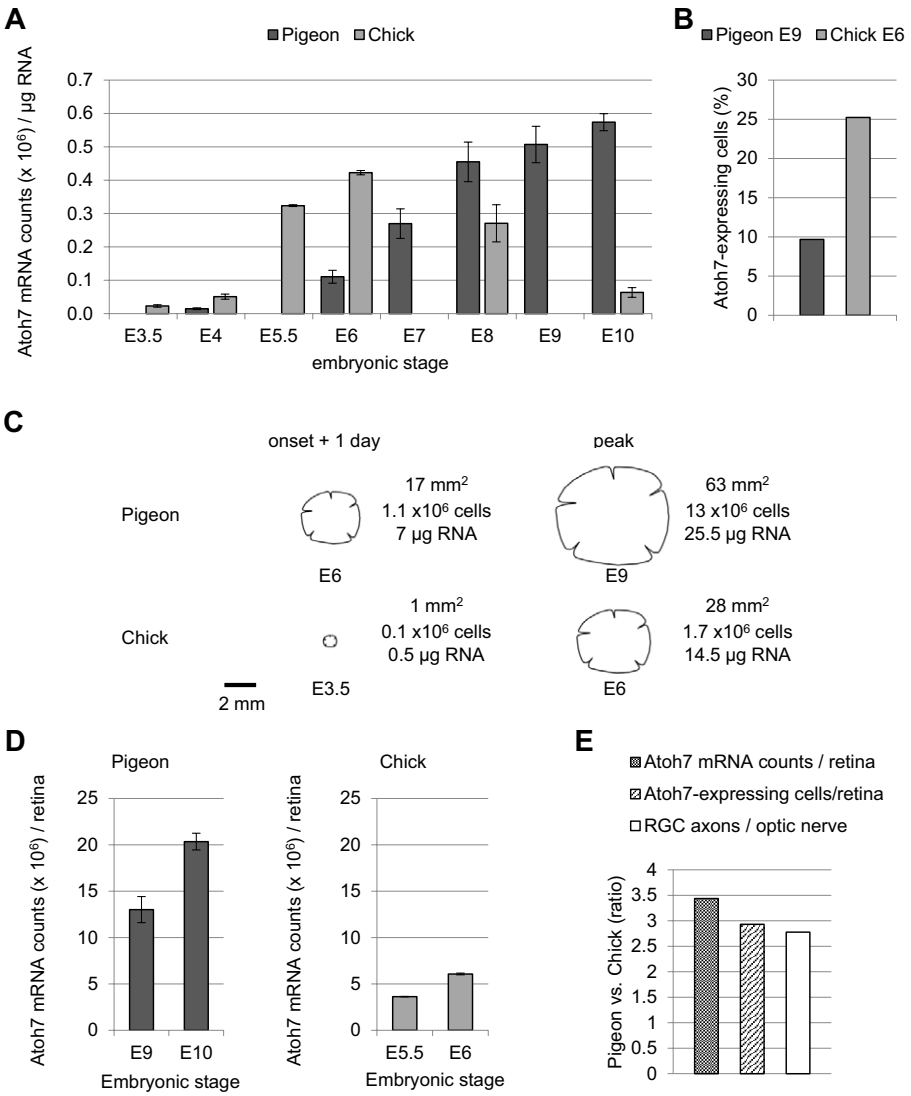

Fig. 5. *Atoh7* transcript counts in pigeon and chick retina. (A) *Atoh7* transcripts were counted using the nCounter analysis system. (B) Fraction of cells that enter the RGC lineage. E6 chick and E9 pigeon retinal cells were transfected with Atoh7-RFP and CMV-GFP. The ratio of RFP^+ to GFP^+ cells was measured 24 h later. (C) Comparison of growth parameters of the retinas 1 day after the onset and at the peak of *Atoh7* expression. (D) *Atoh7* transcript counts per retina at the peak of *Atoh7* expression. (E) Ratios of (left) transcript number in pigeon to transcript number in chick at the peak of *Atoh7* expression, (centre) *Atoh7*-expressing cells in pigeon to *Atoh7*-expressing cells in chick at the peak of *Atoh7* expression, and (right) axon number in pigeon to axon number in chick when fully differentiated (E12 in chick, E17 in pigeon; Fig. 3B). (A,D) At each developmental stage, data are from three biological replicates and are presented as mean±s.d.

time of injection, whereas it was diluted in cells that continue to divide (La Vail et al., 1991). The first heavily labelled cells were detected in the GCL and ONL at E6 (Fig. 6D,E), suggesting that the births of RGCs and photoreceptors begin at the same time. The fact that genesis of RGCs and photoreceptors peaked at E8 and E9 and that only rare cells of the GCL and ONL were labelled at E10 suggest that RGCs and photoreceptors [i.e. mainly cones (Querubin et al., 2009)], have largely congruent periods of cell genesis. In chick, by contrast, RGC genesis starts 2-3 days before the appearance of cones in the area centralis (Bruhn and Cepko, 1996; Prada et al., 1991). In the GCL and ONL, labelled cells were detected at similar frequencies in the central, mid-peripheral and peripheral retinas injected at E6, E8 or E9 (Fig. 6C,E). There was no evidence for a spatiotemporal pattern through which RGC and photoreceptor genesis would spread from the central to peripheral retina. In the INL, heavily labelled cells were first detected in the central and mid-peripheral retina at E9 (Fig. 6C), suggesting that the genesis of interneurons and Muller glia occur after that of RGCs and photoreceptors. The fact that very few cells of the INL were labelled in the periphery at E9 (Fig. 6C) suggests that the genesis of cells of the peripheral INL was delayed with respect to that of cells of the central and mid-peripheral INL. Further studies are needed to establish the birth order of interneurons and Muller glia in the pigeon.

While the spatiotemporal pattern of RGC and photoreceptor births in pigeon is different from that described in chick and other animal models, it strongly resembles the temporal overlap between the periods of RGC and cone genesis observed in monkey (La Vail et al., 1991). It appears that the late genesis of RGCs with respect to photoreceptors contributes to establishing the high ratio of RGCs to cones, i.e. it is a specific trait of the pigeon retina (Fig. S2) (Querubin et al., 2009) and primate fovea.

Notch signalling and patterning of the retina

Hairy/enhancer of split 1 protein (HES1) is a Notch effector that is known to prevent premature differentiation of progenitor cells in early development, thereby allowing neuronal progenitor cell maintenance into later stages of development (reviewed by Imayoshi and Kageyama, 2014). HES1 is expressed in the developing retina and it represses *Atoh7* and *Ngn2* expression (Hernandez et al., 2007; Lee et al., 2005; Matter-Sadzinski et al., 2005). We examined whether prolonged expression of HES1 could account for delaying neuronal differentiation in pigeon. Both the RT-qPCR and RNA-Seq data revealed that the downregulation of *Hes1* followed similar kinetics in pigeon and chick (Fig. S4A,D). Hence, in pigeon, unlike in chick, *Hes1* was already downregulated when *Atoh7* peaked (Fig. 3D). Likewise, the players in the Notch

Development (2016) 143, 4701-4712 doi:10.1242/dev.138719

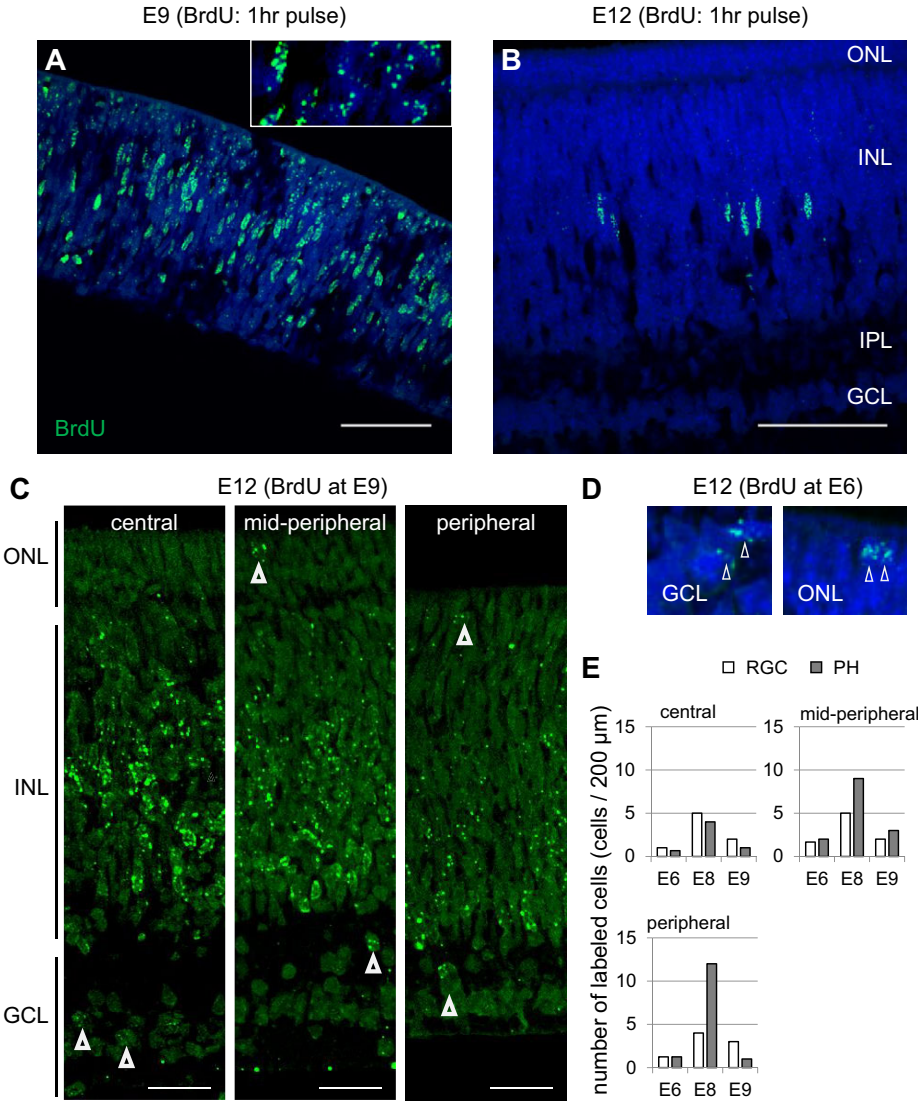

Fig. 6. RGC and photoreceptor genesis in pigeon retina. (A,B) Dissected pigeon retinas were pulse labelled with BrdU for 1 h at E9 (A) and at E12 (B). Transverse sections were processed for immunohistochemistry and counterstained with DAPI. (A) 40±5% of cells are labelled in the central retina. The majority of labelled nuclei display sparse fluorescence puncta (inset). (B) Rare cells are labelled. (C-E) BrdU was injected *in ovo* at E6, E8 or E9. The retinas were then processed for immunohistochemistry at E12. (C) Distribution of labelled cells throughout three areas of the same retina. Arrowheads indicate labelled cells in the GCL and ONL. (D) Daughter cells in the mid-peripheral GCL and ONL. (E) The density of labelled cells (cells per 200 µm retinal length) in the GCL (RGCs) and ONL (PH, photoreceptors) from the centre to the periphery. Scale bars: 50 µm in A,B; 20 µm in C.

signalling pathway, namely *Notch1*, *Notch2*, *Rbpj* and *Jag1* displayed similar expression profiles in pigeon and chick (Fig. S4D). By contrast, expression of the *Hes5* genes was delayed in pigeon (Fig. S4B-D), consistent with the fact that they are activated by ATOH7 (Chiodini et al., 2013). The interplay between ATOH7 and HES5.3 is indeed required for cells to upregulate *Atoh7* and to enter the RGC lineage.

Despite the fact that *Hes5.3* expression is detected in the whole subset of *Atoh7*-expressing progenitor cells, only 25-30% of them upregulate *Atoh7* and enter this lineage in chick between E3 and E5 (Chiodini et al., 2013; Matter-Sadzinski et al., 2005). This low efficiency of RGC production at early stages is attributed to the negative effect of HES1 on *Atoh7 cis*-acting regulatory elements (Hernandez et al., 2007), hence keeping transcription of the *Atoh7* gene at a low level in progenitor cells. Thus, we could expect that, at the onset of *Atoh7* expression in pigeon, a larger subset of cells express *Atoh7* at high levels. To test this idea, E6 pigeon retinas and E3 chick retinas were electroporated with Atoh7-GFP and Atoh7-RFP and fluorescent cells were counted 24 h later. The ratio of red cells to green cells was ∼3-fold higher in pigeon (Fig. 7A). Likewise, the number of *Atoh7* transcripts per microgram of RNA increased ∼4-fold between E6 and E8 in pigeon, whereas it increased ∼14-fold between E3.5 and E5.5 in chick (Fig. 5A), suggesting a vigorous onset of *Atoh7* expression in pigeon.

We wondered whether this reflected an interspecies difference in the patterning of the retina. In E2.5 chick retina, the tiny *Atoh7* and *Ngn2* expression domains coincide in central retina and they abut on the peripheral *Hes1* domain. The concentric expression pattern of *Atoh7* is maintained until E5, and *Hes1* expression, on the whole, remains complementary to that of *Atoh7*, with transcript levels maintained high at the periphery and low in the centre (Matter-Sadzinski et al., 2005). Measurement of *Hes1* expression in tissue fragments dissected in the central and peripheral retina revealed, for both areas, similar transcript levels in pigeon and chick at E6 (Fig. S4A, insets). Under these conditions, *Atoh7* expression peaked throughout the central and peripheral retina in chick (Fig. 4D) (Matter-Sadzinski et al., 2005), whereas it had just started in pigeon. In pigeon, the first cells expressing *Atoh7* at high level were detected throughout the central and peripheral retina at E5.5 and we did not detect any preferential labelling of the central area (Fig. 7B,C). Moreover, in pigeon retinas electroporated with an Atoh7-lacZ reporter plasmid at E6, the β-galactosidase^{+} cells were scattered throughout the central and peripheral retina (Fig. 4C), whereas in chick, at the onset of RGC differentiation at E3, β-galactosidase^{+}

Development (2016) 143, 4701-4712 doi:10.1242/dev.138719

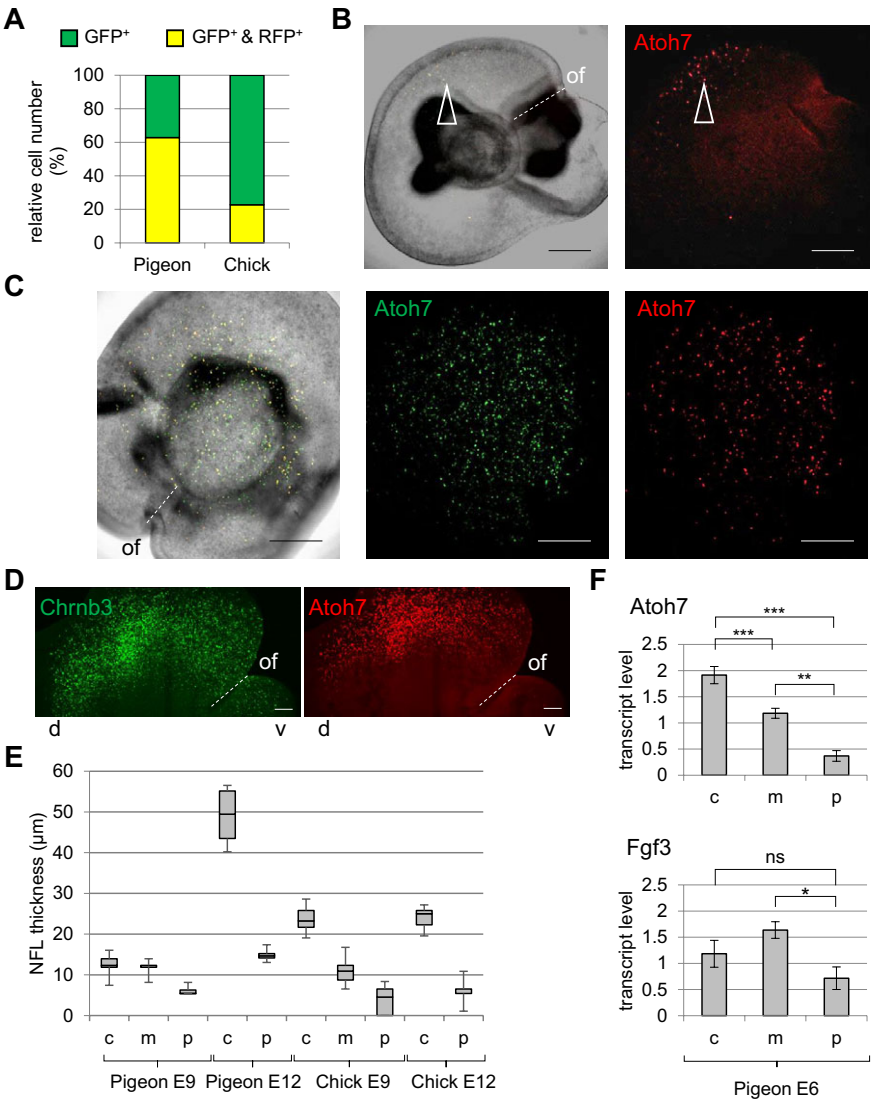

Fig. 7. Spatial patterning of the pigeon retina. (A-C) E4.5 (B), E5 (C) and E6 (A) pigeon retinas and E3 chick retinas (A) were co-electroporated with Atoh7-GFP and Atoh7-RFP. Fluorescent cells were counted 24 h later. (A) Relative numbers of RFP^+ and GFP^+ cells throughout the central and peripheral retina. (B) The first few RFP^+ cells that entered the RGC lineage (arrowhead) are located at the mid-periphery. (C) RFP^+ and GFP^+ cells are uniformly distributed throughout the central and mid-peripheral areas. The peripheral area was not electroporated. The eye lens is apparent by retina transparency. (D) E6 pigeon retina was co-electroporated with Chrnb3-GFP and Atoh7-RFP. Fluorescent cells were detected 48 h later. The overlapping *Chrnb3* and *Atoh7* expression domains encompass the dorsal (d) and ventral (v) retina. The density of *Atoh7*-expressing cells is higher than in C. (E) Box-and-whisker plot illustrating variations in the thickness of the NFL in pigeon and chick retinas at E9 and E12. (F) The accumulation of *Atoh7* and *Fgf3* transcripts was quantified by RT-qPCR in tissue fragments dissected in the central (c), the mid-peripheral (m) and peripheral (p) pigeon retina at E6. Data are from four biological replicates and are presented as mean±s.d. ***P<0.001, **P<0.01, *P<0.05 (Welch's t-test); ns, not significant. Scale bars: 200 µm.

cells are confined to a tiny central domain (Matter-Sadzinski et al., 2005). Consequently, in pigeon, *Chrnb3*, which is an early marker of RGC differentiation and a target of ATOH7 (Chiodini et al., 2013; Skowronska-Krawczyk et al., 2004), is expressed in a domain that encompasses both the ventral and dorsal retina (Fig. 7D). Furthermore, fairly uniform NFL thickness at E9 suggests that, in pigeon, RGCs are produced at the same stage in central and peripheral areas, whereas in chick they emerge in a central-to-peripheral pattern (Fig. 7E). One day after the onset of *Atoh7* expression, *Atoh7* transcripts had accumulated throughout the central and peripheral retina in pigeon (Fig. 7F), whereas they are not yet detectable at the periphery in chick (Matter-Sadzinski et al., 2005). The slightly higher accumulation of *Atoh7* transcripts in the central area at E6 correlates with the increased NFL thickness and enhanced cell density in the GCL of the central retina at E12 (Fig. 7E,F, Fig. S2).

A factor promoting neurogenesis is expressed late in pigeon

To gain insight into the mechanism underlying the late onset of neuronal differentiation in pigeon, we asked if the deferred expression of *Ngn2* and *Atoh7* resulted from a delayed expression of activators. Several members of the fibroblast growth factor (FGF) family are expressed in the developing vertebrate eye and function in optic vesicle patterning and neuronal differentiation (Guillemot and Cepko, 1992; Hyer et al., 1998; Pittack et al., 1997). RNA-Seq and RT-qPCR analysis enabled us to compare the expression profiles of six FGF genes expressed in the course of retinal development.

In each species, *Fgf3* displayed a transient expression profile that coincided with that of *Atoh7* (Fig. S5A). Martinez-Morales et al. (2005) have shown that the concerted activity of FGF3 and FGF8 induces retinal differentiation in chick. In pigeon, *Fgf8* expression peaked ∼2 days before the onset of *Atoh7* expression and it was already downregulated when *Fgf3* was activated (Fig. S5A,B), suggesting that FGF8 was not capable of triggering RGC differentiation by itself. Likewise, *Fgf1* was downregulated at the stages when *Atoh7* was activated and RGCs produced in pigeon (Fig. S5B). Thus, despite the fact that application of exogenous FGF1 induces RGC differentiation in chick (McCabe et al., 1999), FGF3 could well be the best candidate among FGFs for activating neurogenesis in the avian retina (Martinez-Morales et al., 2005). In pigeon, *Fgf3* transcripts accumulated at similar levels in the central and peripheral retina (Fig. 7F). The broad expression domain of *Fgf3* at the time when the first RGCs differentiate could explain, at least in part, the absence of a central-to-peripheral gradient in RGC genesis (Fig. 6C-E).

Development (2016) 143, 4701-4712 doi:10.1242/dev.138719

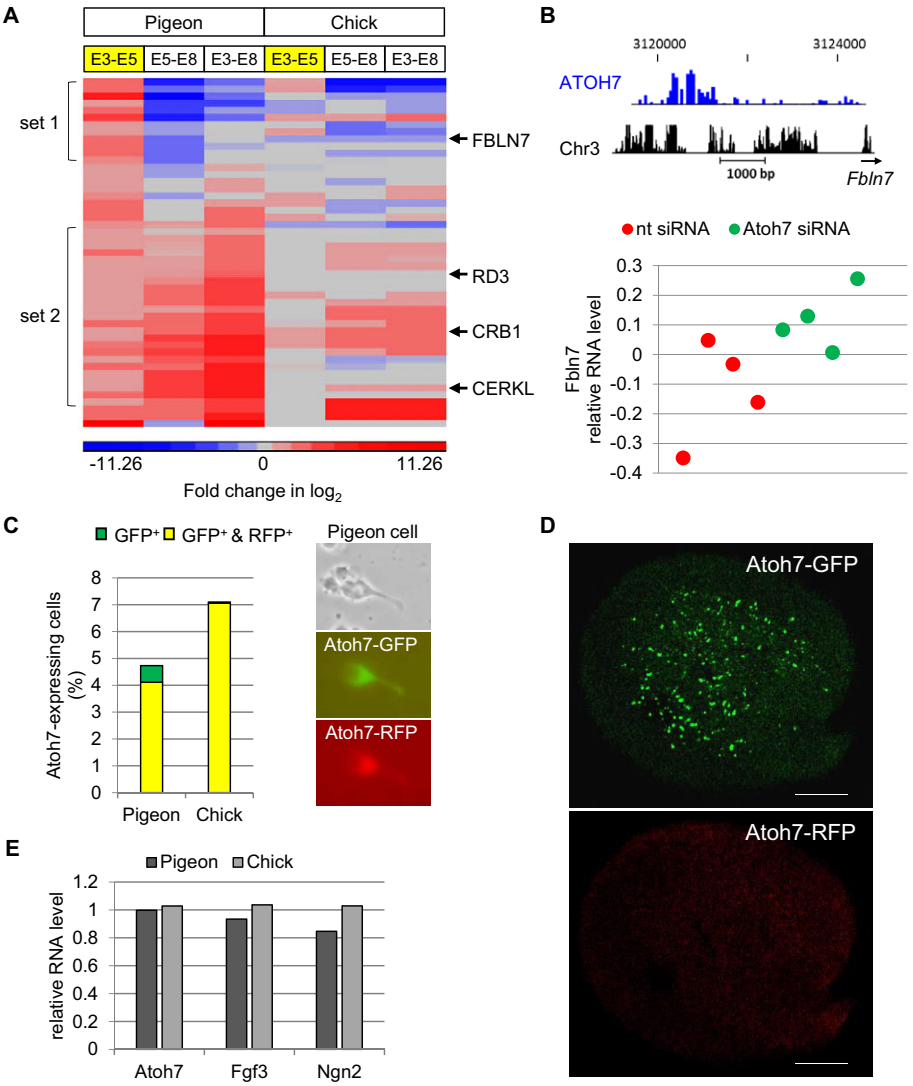

Fig. 8. The pigeon retinal epithelium is inhibitory to RGC differentiation. (A) Heat maps generated from RNA-Seq data showing clustered pigeon genes that display positive fold changes (≥1 in $\log_2$) between E3 and E5 and for which changes in expression of chicken orthologues are not significant during this period. (B) (Top) The chromatin region upstream of *Fbln7* is bound by ATOH7 in E3.5 chick retina. A ~2 kb sequence upstream of *Fbln7* was tiled at 100 bp intervals and the probe coordinates were processed through the UCSC genome browser. (Bottom) E3.5 retinas were electroporated with *Atoh7* siRNAs or non-targeting (nt) siRNAs. Retina fragments were dissected 36 h later and RNA was isolated. The microarray analysis was run in quadruple for each species of siRNAs. ChIP-Chip and microarray data are from experiments reported by Chiodini et al. (2013). (C) E3.5 pigeon and chick retina dissociated cells were transfected with Atoh7-RFP and Atoh7-GFP. (Left) The ratios of RFP^+ and GFP^+ cells to total cell number were calculated 24 h after plating. (Right) A double-labelled pigeon cell. (D) The central and mid-peripheral pigeon retina was co-electroporated with Atoh7-GFP and Atoh7-RFP at E4. No RFP^+ cells were detected 24 h later. (E) E3.5 pigeon and chick retinas were dissociated into single cells that were plated on plastic dishes; RNA was isolated 24 h later and the levels of *Atoh7*, *Ngn2* and *Fgf3* transcripts measured by RT-qPCR. (C,E) Data are from two biological replicates and are presented as the mean. Scale bars: 200 µm.

The pigeon retinal epithelium is inhibitory to RGC differentiation

In pigeon, RGCs are produced, much like in the primate perifoveal area, at the end of the period of cell proliferation, whereas in the chick retina and in the primate peripheral retina, RGCs are produced days and weeks, respectively, ahead of the cessation of cell division (La Vail et al., 1991; Provis et al., 1985). In this context, we examined whether the pigeon retinal epithelium develops special features during the period that precedes the onset of neurogenesis. To address this issue, we selected 49 genes that were activated in pigeon (≥1/N/N) but not in chick (<1/N/N), between E3 and E5. This group includes 13 genes that were upregulated between E3 and E5 and downregulated between E5 and E8 (set 1; Fig. 8A, Table S2). We wondered whether their downregulation was related to the onset of neurogenesis. A ChIP-Chip analysis revealed that ATOH7 protein was bound to sequences upstream of fibulin 7 (*Fbln7*) in E3.5 chick retina (Fig. 8B, top). Electroporation of *Atoh7* siRNAs in chick E3.5 retinas led to the upregulation of *Fbln7* (Fig. 8B, bottom), suggesting that, in pigeon, ATOH7 could repress *Fbln7* between E5 and E8.

FBLN7 is a cell adhesion protein that interacts with extracellular matrix molecules (de Vega et al., 2007). Several other genes encoding matrix, cell adhesion or cytoskeleton components belong to set 1 and we asked if cell-cell interactions in the pigeon retinal epithelium could inhibit cell differentiation. E3.5 pigeon and chick retinas were enzymatically disaggregated, and acutely dissociated cells were co-transfected with Atoh7-RFP and Atoh7-GFP and plated at low density on plastic slides. Similar proportions of pigeon and chick double-labelled cells were detected 24 h after transfection (Fig. 8C), whereas there were no RFP^+ cells in E5 pigeon retinas (Fig. 8D). To verify that cell dissociation abolished the inhibitory effect of the pigeon retinal epithelium on RGC differentiation, E3.5 pigeon and chick dissociated retina cells were plated on plastic dishes and RNA was isolated 24 h later. RT-qPCR analysis revealed that *Atoh7*, *Ngn2* and *Fgf3* transcripts accumulated at the same levels in the pigeon and chick cells (Fig. 8E).

Among the 49 genes that we selected, 23 were activated in pigeon between E3 and E8 (set 2; Fig. 8A, Table S2). None of these genes is involved in retina growth; rather, they might set the ground for the development of retinas of increased complexity resulting from high RGC density, i.e. that bear structural and functional similarities to the primate macula. The fact that genes associated with human retinopathies, such as Leber congenital amaurosis (*Rd3*, *Crb1*) or retinitis pigmentosa (*Cerkl*), belong to this set strengthens the idea that development of the primate macula and pigeon retina share specificities.

Development (2016) 143, 4701-4712 doi:10.1242/dev.138719

DISCUSSION

In chick and mouse embryos, the onset of retinal neurogenesis starts 1 day after the formation of the optic cup. Neurogenesis is initiated in a tiny domain and proceeds in a wave from the central to the peripheral retina that correlates with the central-to-peripheral appearance of postmitotic cells (reviewed by Agathocleous and Harris, 2009). Here we show that neurogenesis in pigeon starts 4 days after the formation of the optic cup and that cells entering the RGC lineage are scattered throughout the central and peripheral retina. Contrary to what has been observed in animal species studied so far, the onset of neuronal differentiation in pigeon is not restricted to the central domain and the genesis of RGCs and photoreceptors does not propagate to the periphery in a wave-like manner. HES1 controls aspects of the patterning of progenitors in chick and mouse retinas and is required for the closure of the optic cup and stalk (Lee et al., 2005; Matter-Sadzinski et al., 2005; Tomita et al., 1996), a landmark in eye morphogenesis that develops at a similar pace in pigeon and chick. The fact that *Hes1* has already been downregulated throughout the retina at the onset of RGC differentiation could explain, at least in part, the absence of a neurogenic wave in pigeon. *Hes1* and other participants of the Notch signalling pathway display similar expression kinetics in pigeon and chick, suggesting that late neurogenesis in pigeon retina does not result from the prolonged inhibition of *Ngn2* and *Atoh7* by HES1, but rather from a time lag in the expression of activators and, in particular, of FGF3 (Martinez-Morales et al., 2005).

The fact that the pigeon eye is already well developed when ATOH7 induces RGC differentiation indicates that the onset of cell differentiation does not keep pace with overall retinal growth. That retinal growth and cell differentiation may proceed according to separate schedules has not been observed previously because of the early onset of neurogenesis in the retinas of the animal models studied so far. This finding challenges the idea that an increase in the number of cells or in the length of the cell cycle during the course of retinal development may act as a biological clock that coordinates the timing of cell differentiation with tissue growth (reviewed by Cepko, 2014). We note that, although the lengthening of the cell cycle is essential for the production of RGCs in chick, the mechanism underlying this process is initiated by ATOH7 and therefore depends on neurogenesis (Chiodini et al., 2013). By postponing neurogenesis to the end of the period of cell proliferation, while maintaining the peak of *Atoh7* expression at the same level as in chick, the pigeon has developed an effective way of expanding the pool of progenitors out of which cells are selected to enter the RGC lineage.

The development of the pigeon retina might represent the rule, rather than the exception, among birds. Phylogenomic studies indicate that one node at the base of the avian tree splits the neognaths between the Galloanserae (e.g. chicken) and the Neonaves, which regroup 95% of avian species and include the orders Columbiformes (e.g. pigeon) and Passeriformes (Hackett et al., 2008; Prum et al., 2015). Although more than half of all bird species are classified in these two orders, only a handful of passerine retinas have been studied so far. It appears that these birds have a fovea and two rod-free areas with high densities of RGCs, much like in pigeon (Coimbra et al., 2009, 2015).

Heterochrony between neurogenesis and growth has a profound effect on the patterning of the retina and on the ratios of cell types. In pigeon, it results in a high ratio of RGCs to cones (Querubin et al., 2009) and high visual acuity (Coletta et al., 2003; Hodos and Leibowitz, 1977). Delaying neurogenesis in the developing CNS might serve different purposes. For instance, the onset of neurogenesis in the telencephalon is delayed in primates compared with rodents, allowing for greater expansion of the founder neural cell pool before neurogenesis begins (reviewed by Florio and Huttner, 2014). In the same manner, most of the post-hatching brain growth in parrots and songbirds is due to a late expansion of the telencephalon, which is associated with a general delay of neurogenesis (Charvet and Striedter, 2011).

Cell proliferation, the expansion and folding of the retinal epithelium, the closure of the optic fissures and the formation of the optic disc all proceed at similar paces in pigeon and chick, in sharp contrast with the respective timings of neuronal differentiation. Twelve TFs and transcriptional regulators that we examined display the same expression profiles in pigeon and chick, suggesting that their role in retinal growth and morphogenesis is independent of cell differentiation. The fact that *Pax2* and *Hes1* belong to this set strengthens the idea that the closure of the optic fissure and optic disc formation are regulated independently of cell differentiation. In humans, the loss of *ALX1* or mutations in *SOX2* lead to craniofacial dysplasia characterised, among other defects, by microphthalmia (Fantes et al., 2003; Taranova et al., 2006; Uz et al., 2010), while in birds the *Alx1* haplotype contributes to diversification of beak shapes among Darwin's finches (Lamichhaney et al., 2015). Similar expression dynamics of *Alx1* and *Sox2* in pigeon and chick highlights how the growth of the retina is coordinated with the increase in eye size and face development irrespective of the time of onset of neurogenesis.

Our study raises two intriguing questions. First, the nature of the signal that lies upstream of the earliest known activators of neurogenesis and how this signal is acting independently of the retinal growth stage. We show that in pigeon the retinal epithelium exerts an inhibitory effect on cell differentiation until the end of the period of cell proliferation and we identified genes encoding matrix, cell adhesion or cytoskeleton components that may participate in this inhibition. Future studies should clarify how these components affect signalling and how they influence the onset of neurogenesis. In optic cups developing *in vitro* from mouse or human embryonic stem cells, RGCs have been identified after 9 and 24 days, respectively, in culture (Eiraku et al., 2011; Nakano et al., 2012). The late onset of cell differentiation in the human optic cup is consistent with the fact that in the primate embryonic retina, RGCs differentiate in the incipient perifoveal area at the end of the period of cell proliferation (Hendrickson, 2016; La Vail et al., 1991; Provis et al., 1985). It remains to be seen whether, in the central area of the primate retina, the epithelium exerts, as in pigeon, an inhibitory effect on neuronal differentiation.

That genes associated with human retinopathies are activated before the onset of cell differentiation in pigeon is intriguing. Very little is known about the function of the proteins that these genes encode, nor do we know whether they are expressed early in foetal human retina. The fact that variants of *ATOH7* could be associated with glaucoma (reviewed by Sakurada and Mabuchi, 2015) highlights how early variations in retina development may eventually lead to retinal diseases later in life. In this context, the pigeon retina could prove to be a useful new model system with which to uncover some of the intricate mechanisms underlying growth and neurogenesis in the macula of primates.

MATERIALS AND METHODS

Animals

Fertilised chicken eggs were from a White Leghorn strain (UNIGE Animal Resources Centre). Fertilised pigeon eggs were supplied by Philippe Delaunay (Pigeonneau de la Suisse Normande, Croisilles, France).

Development (2016) 143, 4701-4712 doi:10.1242/dev.138719

Experimental procedures were carried out in accordance with Federal Swiss Veterinary Regulations.

Molecular cloning

Atoh7 (Atoh7-RFP, Atoh7-GFP, Atoh7-lacZ), *Chrnb3* (Chrnb3-GFP) and CMV-GFP reporter plasmids are described in the supplementary Materials and Methods.

RNA-Seq

RNA samples were isolated in triplicate from pigeon and chick retinas at E3-E3.5, E5-E5.5 and E8-E8.5 and the 18 samples were processed for transcriptome analysis by RNA-Seq. mRNA library preparation and sequencing were performed under contract with Fasteris (Plan-les-Ouates, Switzerland). Stranded-mRNA libraries were prepared from 1 µg total RNA using the TruSeq Stranded mRNA Library Preparation Kit (Illumina) following the manufacturer's instructions. Libraries were sequenced on an Illumina HiSeq 2500 using the TruSeq Rapid SBS Kit (Illumina) and HiSeq Rapid Run (RR) mode, with 150 bp single-end reads. The runs generated 14-24 million reads per sample, of which 69±8% were mappable to reference genomes. Mapping raw reads to reference chick and pigeon genomes was performed using TopHat 2/Bowtie 2 (Kim et al., 2013). Chicken genome reference (WASHUC2 assembly) was obtained from Ensembl.org. Pigeon genome and transcript annotation reference files (assemblies from 2014-02-18) were obtained from the $(GIGA)^n$ database (gigadb.org). Scoring transcript abundances and identification of differentially expressed transcripts was performed using Cufflinks and Cuffdiff scripts from the Cufflinks package (Trapnell et al., 2012). For differential expression, each comparison included data from three biological replicates of either developmental stage.

Northern blot and RT-qPCR

RNA isolated from pigeon and chicken whole and dissected retinas was subject to northern blot analysis with *Hes5.3* and *Atoh7* riboprobes. RT-qPCR was performed using the primers listed in Table S3. For details, see the supplementary Materials and Methods.

NanoString nCounter

To estimate *Atoh7* transcript number, total RNA was subject to NanoString analysis using the probes listed in Table S3. Details are provided in the supplementary Materials and Methods.

Retina morphometric measurements

Retinas from E4 to E17 embryos were dissected, unfixed flat-mounts were photographed and surfaces were measured with ImageJ (NIH). For cell counting, retinas were dissociated as described by Matter-Sadzinski et al. (2005). Cells were counted in a Neubauer chamber. For histology, the retinas and optic nerves were fixed overnight in Trump's 4F:1G fixative (McDowell and Trump, 1976) and embedded in an epoxy resin. Semi-thin sections (1 µm) were stained with Toluidine Blue. Ultra-thin sections (100 nm) at a distance of 0.5-1.0 mm from the optic disc were processed for electron microscopy on an FEI Tecnai G2 Sphera. We used a grid scanning strategy, moving the picture field from the centre of a mesh to the centre of the next to take representative pictures of the whole axon section. Twenty pictures were taken for E10 optic nerve and 46 for E17. Axons were counted in randomly selected 10.76 µm×10.76 µm fields ($n \geq 30$). The number of axons was related linearly to the optic nerve surface (~0.28 mm^2 at E10, ~0.59 mm^2 at E17). Confocal microscopy of retina and single cells is described in the supplementary Materials and Methods.

Retina electroporation and lipofection assay

The electroporation of pigeon and chick retinas with reporters or siRNA, and the transfection of single cells dissociated from chick and pigeon retinas, were performed as detailed in the supplementary Materials and Methods.

BrdU and *lacZ* staining

Cell proliferation was assessed by *in ovo* injection or pulse labelling with BrdU as described in the supplementary Materials and Methods. Atoh7-lacZ reporter activity was assessed as described in the supplementary Materials and Methods.

Acknowledgements

We are grateful to P. Delaunay for the weekly supply of pigeon eggs and for access to embryonic (E14, E15, E16, E17) and adult retinas; and M. Ballivet, T. Halazonetis, B. Galliot and D. Picard for inspiring discussions and critical reading of the manuscript. Confocal and electron microscopy were performed at the Bioimaging Platform of the Faculty of Sciences, University of Geneva. RT-qPCR and NanoString nCounter experiments were performed at the iGE3 Genomics Platform of the University of Geneva.

Competing interests

The authors declare no competing or financial interests.

Author contributions

T.R., L.M.-S. and J.-M.M. carried out experiments. T.R., M.K. and J.-M.M. processed and analysed the data. D.S.-K. provided the ChIP data and participated in data analysis. T.R. and J.-M.M. conceived the study. J.-M.M. and L.M.-S. wrote the manuscript.

Funding

The Swiss National Science Foundation (Schweizerischer Nationalfonds zur Förderung der Wissenschaftlichen Forschung) [grant 31003A-149458], the Gelbert Foundation, the Velux Foundation (Velux Stiftung), the Fonds Suisse pour la prévention et la lutte contre la cécité, and the state of Geneva support our laboratory.

Data availability

Unpublished histological data concerning the pigeon retina and optic nerve are available at http://www.genes-vision.ch/pigeon. RNA-Seq data have been deposited at Gene Expression Omnibus under accession number GSE89541.

Supplementary information

Supplementary information available online at
http://dev.biologists.org/lookup/doi/10.1242/dev.138719.supplemental

References

Agathocleous, M. and Harris, W. A. (2009). From progenitors to differentiated cells in the vertebrate retina. *Annu. Rev. Cell Dev. Biol.* **25**, 45-69.

Brown, N. L., Kanekar, S., Vetter, M. L., Tucker, P. K., Gemza, D. L. and Glaser, T. (1998). Math5 encodes a murine basic helix-loop-helix transcription factor expressed during early stages of retinal neurogenesis. *Development* **125**, 4821-4833.

Brown, N. L., Patel, S., Brzezinski, J. and Glaser, T. (2001). Math5 is required for retinal ganglion cell and optic nerve formation. *Development* **128**, 2497-2508.

Bruhn, S. L. and Cepko, C. L. (1996). Development of the pattern of photoreceptors in the chick retina. *J. Neurosci.* **16**, 1430-1439.

Cepko, C. (2014). Intrinsically different retinal progenitor cells produce specific types of progeny. *Nat. Rev. Neurosci.* **15**, 615-627.

Charvet, C. J. and Striedter, G. F. (2011). Developmental modes and developmental mechanisms can channel brain evolution. *Front. Neuroanat.* **5**, 4.

Chen, Y. and Naito, J. (1999). A quantitative analysis of cells in the ganglion cell layer of the chick retina. *Brain Behav. Evol.* **53**, 75-86.

Chiodini, F., Matter-Sadzinski, L., Rodrigues, T., Skowronska-Krawczyk, D., Brodier, L., Schaad, O., Bauer, C., Ballivet, M. and Matter, J.-M. (2013). A positive feedback loop between ATOH7 and a Notch effector regulates cell-cycle progression and neurogenesis in the retina. *Cell Rep.* **3**, 796-807.

Coimbra, J. P., Trévia, N., Videira Marceliano, M. L., da Silveira Andrade-Da-Costa, B. L., Picanço-Diniz, C. W. and Yamada, E. S. (2009). Number and distribution of neurons in the retinal ganglion cell layer in relation to foraging behaviors of tyrant flycatchers. *J. Comp. Neurol.* **514**, 66-73.

Coimbra, J. P., Collin, S. P. and Hart, N. S. (2015). Variations in retinal photoreceptor topography and the organization of the rod-free zone reflect behavioral diversity in Australian passerines. *J. Comp. Neurol.* **523**, 1073-1094.

Coletta, N. J., Marcos, S., Wildsoet, C. and Troilo, D. (2003). Double-pass measurement of retinal image quality in the chicken eye. *Optom. Vis. Sci.* **80**, 50-57.

Conradi, N. and Sjöstrand, J. (1993). A morphometric and stereologic analysis of ganglion cells of the central human retina. *Graefes Arch. Clin. Exp. Ophthalmol.* **231**, 169-174.

de Vega, S., Iwamoto, T., Nakamura, T., Hozumi, K., McKnight, D. A., Fisher, L. W., Fukumoto, S. and Yamada, Y. (2007). TM14 is a new member of the fibulin family (fibulin-7) that interacts with extracellular matrix molecules and is active for cell binding. *J. Biol. Chem.* **282**, 30878-30888.

Development (2016) 143, 4701-4712 doi:10.1242/dev.138719

Del Bene, F., Ettwiller, L., Skowronska-Krawczyk, D., Baier, H., Matter, J.-M., Birney, E. and Wittbrodt, J. (2007). In vivo validation of a computationally predicted conserved Ath5 target gene set. *PLoS Genet.* **3**, e159.

Duronio, R. J. (2012). Developing S-phase control. *Genes Dev.* **26**, 746-750.

Eiraku, M., Takata, N., Ishibashi, H., Kawada, M., Sakakura, E., Okuda, S., Sekiguchi, K., Adachi, T. and Sasai, Y. (2011). Self-organizing optic-cup morphogenesis in three-dimensional culture. *Nature* **472**, 51-56.

Fantes, J., Ragge, N. K., Lynch, S.-A., McGill, N. I., Collin, J. R., Howard-Peebles, P. N., Hayward, C., Vivian, A. J., Williamson, K., van Heyningen, V. et al. (2003). Mutations in SOX2 cause anophthalmia. *Nat. Genet.* **33**, 461-463.

Florio, M. and Huttner, W. B. (2014). Neural progenitors, neurogenesis and the evolution of the neocortex. *Development* **141**, 2182-2194.

Galifret, Y. (1968). [The various functional areas of the retina of pigeons]. *Z. Zellforsch. Mikrosk. Anat.* **86**, 535-545.

Goldberg, S. and Coulombre, A. J. (1972). Topographical development of the ganglion cell fiber layer in the chick retina. A whole mount study. *J. Comp. Neurol.* **146**, 507-517.

Guillemot, F. and Cepko, C. L. (1992). Retinal fate and ganglion cell differentiation are potentiated by acidic FGF in an in vitro assay of early retinal development. *Development* **114**, 743-754.

Hackett, S. J., Kimball, R. T., Reddy, S., Bowie, R. C. K., Braun, E. L., Braun, M. J., Chojnowski, J. L., Cox, W. A., Han, K.-L., Harshman, J. et al. (2008). A phylogenomic study of birds reveals their evolutionary history. *Science* **320**, 1763-1768.

Hendrickson, A. (2016). Development of retinal layers in prenatal human retina. *Am. J. Ophthalmol.* **161**, 29-35.e1.

Hernandez, J., Matter-Sadzinski, L., Skowronska-Krawczyk, D., Chiodini, F., Alliod, C., Ballivet, M. and Matter, J.-M. (2007). Highly conserved sequences mediate the dynamic interplay of basic helix-loop-helix proteins regulating retinogenesis. *J. Biol. Chem.* **282**, 37894-37905.

Hodos, W. and Leibowitz, R. W. (1977). Near-field visual acuity of pigeons: effects of scotopic adaptation and wavelength. *Vision Res.* **17**, 463-467.

Hufnagel, R. B. and Brown, N. L. (2013). Specification of retinal cell types. In *Patterning and Cell Type Specification in the Developing CNS and PNS* (ed. J. Rubenstein and P. Rakic), pp. 519-537. San Diego: Academic Press.

Hufnagel, R. B., Le, T. T., Riesenberg, A. L. and Brown, N. L. (2010). Neurog2 controls the leading edge of neurogenesis in the mammalian retina. *Dev. Biol.* **340**, 490-503.

Hyer, J., Mima, T. and Mikawa, T. (1998). FGF1 patterns the optic vesicle by directing the placement of the neural retina domain. *Development* **125**, 869-877.

Imayoshi, I. and Kageyama, R. (2014). Oscillatory control of bHLH factors in neural progenitors. *Trends Neurosci.* **37**, 531-538.

Jeon, C. J., Strettoi, E. and Masland, R. H. (1998). The major cell populations of the mouse retina. *J. Neurosci.* **18**, 8936-8946.

Kanekar, S., Perron, M., Dorsky, R., Harris, W. A., Jan, L. Y., Jan, Y. N. and Vetter, M. L. (1997). Xath5 participates in a network of bHLH genes in the developing Xenopus retina. *Neuron* **19**, 981-994.

Kay, J. N., Finger-Baier, K. C., Roeser, T., Staub, W. and Baier, H. (2001). Retinal ganglion cell genesis requires lakritz, a zebrafish atonal homolog. *Neuron* **30**, 725-736.

Kim, D., Pertea, G., Trapnell, C., Pimentel, H., Kelley, R. and Salzberg, S. L. (2013). TopHat2: accurate alignment of transcriptomes in the presence of insertions, deletions and gene fusions. *Genome Biol.* **14**, R36.

Kolb, H. (1995). Midget pathways of the primate retina underlie resolution and red green color opponency. In *Webvision: The Organization of the Retina and Visual System* (ed. H. Kolb, E. Fernandez and R. Nelson). http://webvision.med.utah.edu.

La Vail, M. M., Rapaport, D. H. and Rakic, P. (1991). Cytogenesis in the monkey retina. *J. Comp. Neurol.* **309**, 86-114.

Lamichhaney, S., Berglund, J., Almén, M. S., Maqbool, K., Grabherr, M., Martinez-Barrio, A., Promerová, M., Rubin, C.-J., Wang, C., Zamani, N. et al. (2015). Evolution of Darwin's finches and their beaks revealed by genome sequencing. *Nature* **518**, 371-375.

Lee, H. Y., Wroblewski, E., Philips, G. T., Stair, C. N., Conley, K., Reedy, M., Mastick, G. S. and Brown, N. L. (2005). Multiple requirements for Hes1 during early eye formation. *Dev. Biol.* **284**, 464-478.

Liu, W., Mo, Z. and Xiang, M. (2001). The Ath5 proneural genes function upstream of Brn3 POU domain transcription factor genes to promote retinal ganglion cell development. *Proc. Natl. Acad. Sci. USA* **98**, 1649-1654.

Martinez-Morales, J.-R., Del Bene, F., Nica, G., Hammerschmidt, M., Bovolenta, P. and Wittbrodt, J. (2005). Differentiation of the vertebrate retina is coordinated by an FGF signaling center. *Dev. Cell* **8**, 565-574.

Matter-Sadzinski, L., Matter, J. M., Ong, M. T., Hernandez, J. and Ballivet, M. (2001). Specification of neurotransmitter receptor identity in developing retina: the chick ATH5 promoter integrates the positive and negative effects of several bHLH proteins. *Development* **128**, 217-231.

Matter-Sadzinski, L., Puzianowska-Kuznicka, M., Hernandez, J., Ballivet, M. and Matter, J. M. (2005). A bHLH transcriptional network regulating the specification of retinal ganglion cells. *Development* **132**, 3907-3921.

McCabe, K. L., Gunther, E. C. and Reh, T. A. (1999). The development of the pattern of retinal ganglion cells in the chick retina: mechanisms that control differentiation. *Development* **126**, 5713-5724.

McDowell, E. M. and Trump, B. F. (1976). Histologic fixatives suitable for diagnostic light and electron microscopy. *Arch. Pathol. Lab. Med.* **100**, 405-414.

Nakano, T., Ando, S., Takata, N., Kawada, M., Muguruma, K., Sekiguchi, K., Saito, K., Yonemura, S., Eiraku, M. and Sasai, Y. (2012). Self-formation of optic cups and storable stratified neural retina from human ESCs. *Cell Stem Cell* **10**, 771-785.

Pittack, C., Grunwald, G. B. and Reh, T. A. (1997). Fibroblast growth factors are necessary for neural retina but not pigmented epithelium differentiation in chick embryos. *Development* **124**, 805-816.

Prada, C., Puga, J., Perez-Mendez, L., Lopez, R. and Ramirez, G. (1991). Spatial and temporal patterns of neurogenesis in the chick retina. *Eur. J. Neurosci.* **3**, 1187.

Prasov, L. and Glaser, T. (2012). Pushing the envelope of retinal ganglion cell genesis: context dependent function of Math5 (Atoh7). *Dev. Biol.* **368**, 214-230.

Provis, J. M., Van Driel, D., Billson, F. A. and Russell, P. (1985). Development of the human retina: patterns of cell distribution and redistribution in the ganglion cell layer. *J. Comp. Neurol.* **233**, 429-451.

Prum, R. O., Berv, J. S., Dornburg, A., Field, D. J., Townsend, J. P., Lemmon, E. M. and Lemmon, A. R. (2015). A comprehensive phylogeny of birds (Aves) using targeted next-generation DNA sequencing. *Nature* **526**, 569-573.

Querubin, A., Lee, H. R., Provis, J. M. and O'Brien, K. M. B. (2009). Photoreceptor and ganglion cell topographies correlate with information convergence and high acuity regions in the adult pigeon (Columba livia) retina. *J. Comp. Neurol.* **517**, 711-722.

Rager, G. H. (1980). Development of the retinotectal projection in the chicken. *Adv. Anat. Embryol. Cell Biol.* **63**, I-VIII, 1-90.

Sakurada, Y. and Mabuchi, F. (2015). Advances in glaucoma genetics. *Prog. Brain Res.* **220**, 107-126.

Sinn, R., Peravali, R., Heermann, S. and Wittbrodt, J. (2014). Differential responsiveness of distinct retinal domains to Atoh7. *Mech. Dev.* **133**, 218-229.

Skowronska-Krawczyk, D., Ballivet, M., Dynlacht, B. D. and Matter, J.-M. (2004). Highly specific interactions between bHLH transcription factors and chromatin during retina development. *Development* **131**, 4447-4454.

Skowronska-Krawczyk, D., Chiodini, F., Ebeling, M., Alliod, C., Kundzewicz, A., Castro, D., Ballivet, M., Guillemot, F., Matter-Sadzinski, L. and Matter, J.-M. (2009). Conserved regulatory sequences in Atoh7 mediate non-conserved regulatory responses in retina ontogenesis. *Development* **136**, 3767-3777.

Taranova, O. V., Magness, S. T., Fagan, B. M., Wu, Y., Surzenko, N., Hutton, S. R. and Pevny, L. H. (2006). SOX2 is a dose-dependent regulator of retinal neural progenitor competence. *Genes Dev.* **20**, 1187-1202.

Tomita, K., Ishibashi, M., Nakahara, K., Ang, S.-L., Nakanishi, S., Guillemot, F. and Kageyama, R. (1996). Mammalian hairy and Enhancer of split homolog 1 regulates differentiation of retinal neurons and is essential for eye morphogenesis. *Neuron* **16**, 723-734.

Trapnell, C., Roberts, A., Goff, L., Pertea, G., Kim, D., Kelley, D. R., Pimentel, H., Salzberg, S. L., Rinn, J. L. and Pachter, L. (2012). Differential gene and transcript expression analysis of RNA-seq experiments with TopHat and Cufflinks. *Nat. Protoc.* **7**, 562-578.

Uz, E., Alanay, Y., Aktas, D., Vargel, I., Gucer, S., Tuncbilek, G., von Eggeling, F., Yilmaz, E., Deren, O., Posorski, N. et al. (2010). Disruption of ALX1 causes extreme microphthalmia and severe facial clefting: expanding the spectrum of autosomal-recessive ALX-related frontonasal dysplasia. *Am. J. Hum. Genet.* **86**, 789-796.

Wang, S. W., Kim, B. S., Ding, K., Wang, H., Sun, D., Johnson, R. L., Klein, W. H. and Gan, L. (2001). Requirement for math5 in the development of retinal ganglion cells. *Genes Dev.* **15**, 24-29.

Williams, D. R. (1985). Visibility of interference fringes near the resolution limit. *J. Opt. Soc. Am. A* **2**, 1087.

Yang, Z., Ding, K., Pan, L., Deng, M. and Gan, L. (2003). Math5 determines the competence state of retinal ganglion cell progenitors. *Dev. Biol.* **264**, 240-254.